

An Extrapolation Method Based on Current for Rapid Frequency and Angle Sweeps in Far-Field Calculation in an Integral Equation Algorithm⁺

C. C. Lu

Department of Electrical Engineering
University of Kentucky
Lexington, KY 40506
cclu@engr.uky.edu

Abstract: An extrapolation method based on the solution of induced current is introduced to rapidly perform angle and frequency sweep in the far-field calculation using the sparsely sampled solutions. This method is based on the observation of the characteristics of the current distribution as a function of incident angles and frequency. It is easy to be implemented for in-core processing, and needs a small extra memory. In addition, the extrapolation applies to both angle and frequency sweeps. Numerical examples for conducting and material scatterers show that the far-field scattering results generated by the extrapolation method agree to that provided by the direct solution, but the extrapolation method uses about the same amount of memory, and much less CPU time than that of the brute-force approach.

I. Introduction

The algorithms based on the iterative solution of the integral equations and accelerated by fast solvers provide efficient and accurate ways to calculate the scattering by large and complex objects. The application of the fast solvers such as the multilevel fast multipole algorithm [1] has greatly reduced the computational complexity of a matrix vector multiplication for the iteration process. To further increase the efficiency in producing multi-angle and multi-frequency scattering data, attentions are focused on (a) developing precondition techniques to reduce the number of iterations for a converged solution, (b) developing advanced post processing methods which use the information of the existing solution to predict as much scattering data as possible. Several algorithms have been studied such as the frequency interpolation on current or scattered field, and the bi-static to mono-static

approximation [2, 3, 5-10].

For frequency loop acceleration, a straight forward method is to perform interpolation using the scattered field samples that are obtained directly via a numerical solver. This method is simple in implementation, but it applies to densely sampled scattered field only, and has poor prediction accuracy if applied to frequencies outside the frequency samples. A more sophisticated algorithm exploits the characteristics of scattered field vs the frequency. Basically, it assumes that scattered field at a given frequency can be written as a series of exponentials. This method tries to estimate the expansion coefficients using a set of scattering field samples. Since only the field samples are used, it can be implemented out of core (i.e., it can be performed when all the field samples are available). This method can also be applied to the induced current. In this case, the induced current at target mesh samples must be saved for every frequency samples, leading to increased memory requirement and processing CPU time for in-core processing.

For angle loop acceleration, there are also similar methods as above. One of the popular and effective methods is the approximation of mono-static RCS using bi-static results. This method was originally applied to process the measurement RCS data where the exact mono-static configuration is difficult to realize.

In this paper, an approximate extrapolation method is introduced to rapidly fill the angular and frequency far-field points using the solutions at sparsely sampled points. This method is based on the characteristics of the induced current on the target surface. It assumes that the leading term of

⁺ This work was supported in part by the Office of Naval Research under Award No. N00014-00-1-0605, and in part by National Science Foundation under award No. ECS-0093692.

the induced current at every surface depends on the frequency and incident angles via a complex exponential function. With this assumption, the solution at a fixed angle can be processed by replacing the angle dependency factor with a similar factor for the new incident angles. This process is called “normalization”. One advantage of this method is that the normalization can be performed for angle variables as well as frequency. In the following, the exponential dependency is first verified from the point of view of the method of moment solution. Then numerical verification and application examples are provided. The time factor used in this paper is $\exp(-i\omega t)$ and is suppressed from the equations.

II. Formulation

The following derivation is for a three-dimensional perfectly conducting scatterer. The procedure can also be applied to scatterers of dielectric material and material coating on conducting object. In fact, in Sec. 3, there is an example that shows the application of extrapolation to material coated object. Consider the discretization of the surface integral equation for a scattering problem by the method of moments. For simplicity, it is assumed that the target surface is divided into a set of patches, each of which has dimension of one tenth of a wavelength. The induced current on the target surface is represented by a set of N basis functions. Each basis function $\tilde{f}_n(\vec{r})$ is defined for an interior edge, which is shared by two patches. Following the standard MoM procedure with Galerkin testing scheme, a set of linear algebra equations is obtained as

$$\sum_n Z_{mn} a_n = V_m \quad (1)$$

where, Z_{mn} is an impedance matrix element, a_n is an expansion coefficient for basis function $\tilde{f}_n(\vec{r})$, and V_m is an element of excitation vector that is related to the excitation field \vec{E}^{inc} (also called incident field) as

$$V_m = - \int_{S_m} \tilde{f}_m(\vec{r}) \cdot \vec{E}^{inc}(\vec{r}) dS. \quad (2)$$

For a plane wave incidence at direction \hat{k}^i , $\vec{E}^{inc} = \vec{E}_0 \exp(i\vec{k}^i \cdot \vec{r})$, where $\vec{k}^i = k_0 \hat{k}^i$, and k_0 is the free-space wave number. Using a numerical

quadrature rule to approximately evaluate (2) gives rise to

$$\begin{aligned} V_m &= \sum_q w_q [-\tilde{f}_m(\vec{r}_q)] \cdot \vec{E}_0 e^{i\vec{k}^i \cdot \vec{r}_q} \\ &= e^{i\vec{k}^i \cdot \vec{r}_m} \sum_q w_q [-\tilde{f}_m(\vec{r}_q)] \cdot \vec{E}_0 e^{i\vec{k}^i \cdot (\vec{r}_q - \vec{r}_m)}. \end{aligned}$$

In the above equation, \vec{r}_m is the center position of basis- m , w_q is the weighting coefficient, \vec{r}_q is the quadrature point that lies inside the domain s_m of basis- m . Since $|\vec{r}_q - \vec{r}_m|$ is at most of the size of the domain which is about two tenth of the wavelength, the factor $\exp(i\vec{k}^i \cdot (\vec{r}_q - \vec{r}_m))$ is a slow varying function of frequency and angle. Also, \vec{E}_0 , w_q , and the test function \tilde{f}_m are not functions of angle and frequency. As a result, the excitation element V_m can be written as

$$V_m = \tilde{V}_m e^{i\vec{k}^i \cdot \vec{r}_m} \quad (3)$$

where \tilde{V}_m is a slow varying function of frequency and incident angle. If the system of equations in (1) is inverted symbolically and the right hand side in (3) is used to replace V_m in (1), then the solution for the unknown expansion coefficient a_n will be given by

$$\begin{aligned} a_n &= \sum_m [Z^{-1}]_{nm} \tilde{V}_m e^{i\vec{k}^i \cdot \vec{r}_m} \\ &= e^{i\vec{k}^i \cdot \vec{r}_n} \sum_m [Z^{-1}]_{nm} \tilde{V}_m e^{i\vec{k}^i \cdot (\vec{r}_m - \vec{r}_n)} \end{aligned} \quad (4)$$

where $[Z^{-1}]_{nm}$ is an element of the inverse impedance matrix. It is known that the impedance matrix elements are related to the 3D Green's function, hence it contains the factor of $\exp(ik_0|\vec{r}_m - \vec{r}_n|)$. As a result, if \vec{r}_n is close to \vec{r}_m , it is a slow varying function of frequency (it is not a function of incident angles) compared to the factor of $\exp(i\vec{k}^i \cdot \vec{r}_n)$. For the exponential factor $\exp(i\vec{k}^i \cdot (\vec{r}_m - \vec{r}_n))$ in (4), it is also a slow varying function of frequency and angle if \vec{r}_n is close to \vec{r}_m . If the two positions are far away, this factor becomes a rapidly varying function of frequency and angles. However, for most of the elements, the interaction becomes weaker when they are far from each other (there are exceptions that will be stated later in the numerical result sections). As a

result, it is concluded that

$$a_n = \tilde{a}_n e^{i\vec{k}^i \cdot \vec{r}_n}, \quad (5)$$

where \tilde{a}_n is a slow varying function of frequency and angles for most of the elements. In the following, \tilde{a}_n is called the normalized coefficient, and a_n is the un-normalized coefficient. Based on this observation, the solution of the current coefficient for the same basis function for any near-by incident plane wave \vec{k}_2^i can be approximated by $\tilde{a}_n \exp\{i(\vec{k}_2^i + \vec{\Delta}^i) \cdot \vec{r}_n\}$. In this expression, $\vec{\Delta}^i = \vec{k}_2^i - \vec{k}_1^i$ is small in magnitude, and it represents the small shift in frequency and angles from the previous plane wave with \vec{k}_1^i . Since the induced current at a point in a patch is a superposition of the basis functions that are associated with that patch, the current solution has the same expression as (4), i.e., $J(r) = \tilde{J}(\vec{r}) \exp(i\vec{k}^i \cdot \vec{r})$, where $\tilde{J}(\vec{r})$, a component of surface induced current, is a slow varying function

of frequency and angle, but it is a function of position.

To demonstrate the above observations, consider a target that is made by five spheres that are uniformly placed on x-axis, each of which has radius of 0.3 m, as shown in Figure 1. The center distance between two neighbor spheres is 0.45 m. The spheres are discretized into 3,000 quadrilateral patches. The frequency of the incident plane wave is 1 GHz and is vertically polarized. Figure 2 shows the solution for basis number 1345 which is centered at (0,0.18,0). It can be seen that the normalized coefficient (dash lines) is indeed varying slowly with incident angle ϕ^i compared to the un-normalized version of the same coefficient (the solid lines). Because of this property of the normalized coefficient, it can be accurately represented by a linear interpolation for a large angular range.

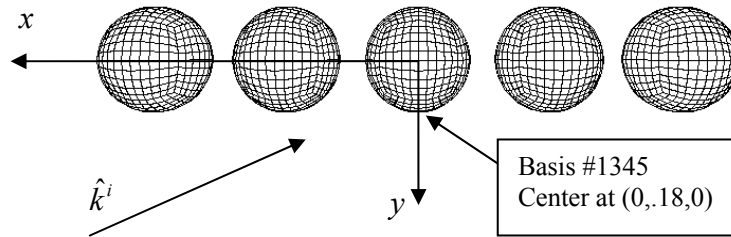


Figure 1. Five conducting spheres on x-axis. Each sphere has radius 0.3m, and the center distance of two neighbor spheres is 0.45 m.

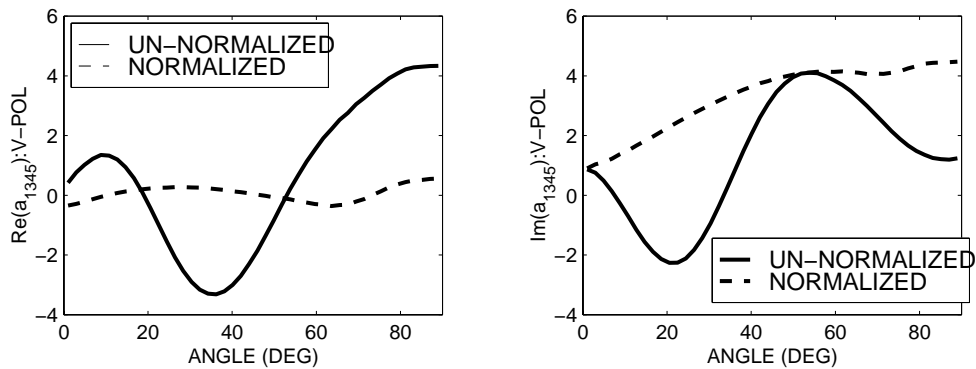


Figure 2. The real part (left) and imaginary part (right) of the solution for basis number 1345. The incident angle $\theta^i = 90^\circ$, and the horizontal variable ϕ^i varies from 0° to 90° .

The implementation of the current extrapolation is straightforward. It only involves two steps. First the system of equations (1) is solved to obtain the coefficient for one angle/frequency sample. From this solution, the normalized coefficient is extracted using equation (4). Then, in the second step, the normalized coefficient is multiplied by a correction factor of $\exp(i(\vec{k}^i + \vec{\Delta}) \cdot \vec{r}_n)$ to obtain the basis function coefficient for any near-by frequency and angle samples.

III. Numerical Results

In this section, examples will be shown to demonstrate the application of the current extrapolation method. The results are generated using a multilevel fast multipole algorithm [11] that is implemented for the solution of hybrid surface-volume integral equations [1]. The first example shows the comparison of the RCS for the five-sphere target given in Figure 1. The results are plotted in Figure 3 for the V-V and H-H polarized incident cases. It can be seen that the extrapolated results using five samples are very close to that obtained by brute-force method (in which, the solution to the system equation is obtained for every incident angles). In the plot of Figure 3, the horizontal axis AZ is defined as $-\phi^i$.

The second example consists of a simple airplane model that is made by two conducting plates (as wings) attached to a cone-cylinder-hemisphere structure. The mesh description is shown in Figure 4 and the radar cross sections as function of frequency, calculated using the brute-force approach (solution for every point of RCS output) and the extrapolation method, are shown in Figure 5. The mono-static angles for this result are $\theta^i = 30^\circ$, $\phi^i = 30^\circ$.

The third example considers scattering of a model airplane VFY218 [1] at 300 MHz. Figure 6 shows the comparison of the 361 RCS points (0.5

degrees step size) on the horizontal plane (0° – 180° range) using (1) the brute-force approach which calculates the solution for every output point (the solid dots), (2) the current extrapolation method of this paper (the solid line) using the solutions at the sampling points (the circles), and (3) the bi-static to mono-static approximation method provided in [3] (the dash line). In both of the two approximations ((2) and (3)), the number of sampling angles is 31. This sampling rate is determined by the approximate formula that the angle increments between two neighbor samples is $25\sqrt{\lambda/D}$, with D being the target's physical dimension. It can be seen that the agreements of the approximate methods with the direct solution are reasonably well.

It should be pointed out that the overall saving of the CPU time is slightly smaller than the ratio of the numbers of the dense sample (brute-force solution) and the sparse sample (for extrapolation). For example, in the VFY218 example introduced above, the CPU time for the direct solution of all output points is 12.03 hours on a HP Supercomputer, and the CPU times for both of the two approximate methods are 142 minutes, and 138 minutes, respectively (a theoretically expected values for the approximate method would be 120 minutes which is 6 times less than that of the brute-force approach). The reason behind the phenomena is the increased iteration number for the same convergence criterion in the brute-force solution and the extrapolation. The algorithm used in generating the data of the above examples employed an implementation for the iteration, in which the solution from the previous incidence is applied to approximate the initial guess of the next incident point. It is known that the denser the solution samples, the closer the two solutions of the adjacent sampling points.

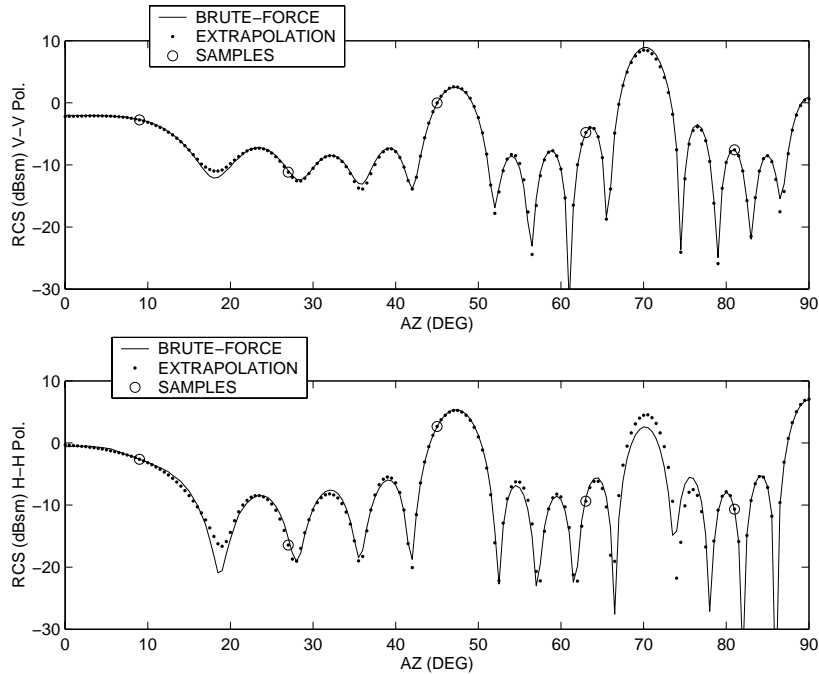


Figure 3. The comparison between brute-force solution and extrapolation for the RCS of the five conducting spheres shown in Figure 1.

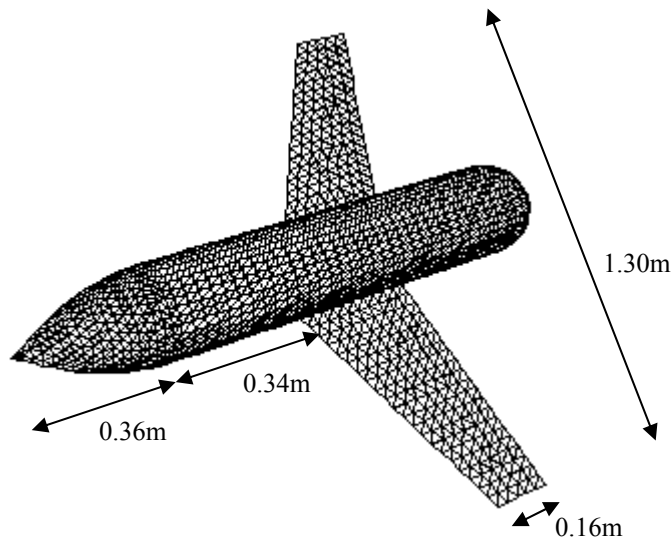


Figure 4. An airplane-like model made of 5 pieces: two trapezoidal plates (as wings), a cone, a circular cylinder, and a hemisphere. The cone's profile is parabolic with height 0.36 m, the radius of the circular cylinder and the hemisphere tail is 0.12 m, the length of the cylindrical part is 1.0 m, the two plates are identical in shape and size, the two parallel sides are 0.32 m and 0.16 m, respectively. The other parameters are shown in the sketch.

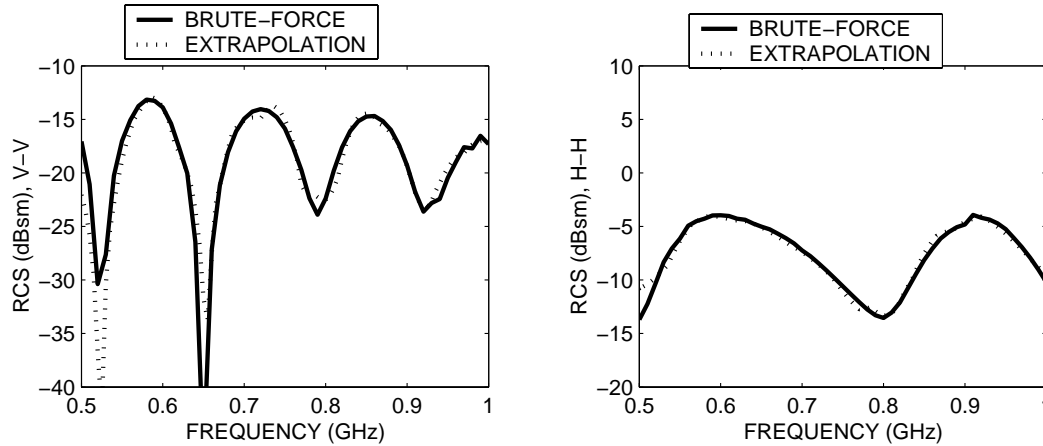


Figure 5. The comparisons of RCS that is directly calculated and extrapolated for the simple airplane model in Figure 4. The number of frequency samples used to generate the extrapolated result is 10.

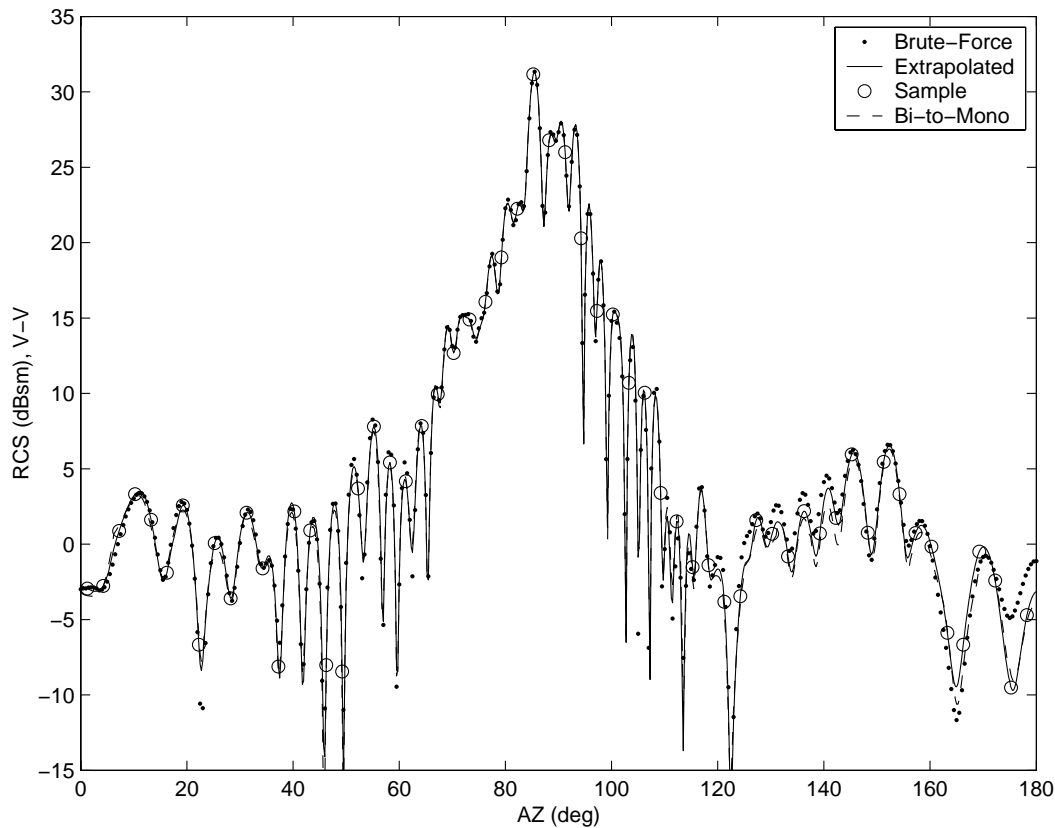


Figure 6. The directly calculated (brute-force) and the extrapolated RCS results of VFY 218 at 300 MHz in the horizontal plane ($\theta^i = 90^\circ$). The circles indicate the sampling points from which the RCS of the dense output points (the solid line) are generated. The dot-dash line is the result using the bi-static to mono-static approximation method.

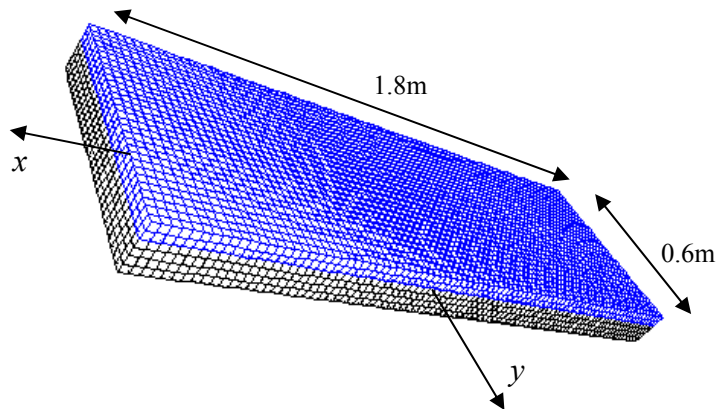


Figure 7. A conducting box with dielectric coating. The thickness of the box (bottom part) is 0.08 m, and the coating slab thickness is 0.04 m. The number unknowns for the conducting part is 12720, and the number of unknowns for the material part is 19140.

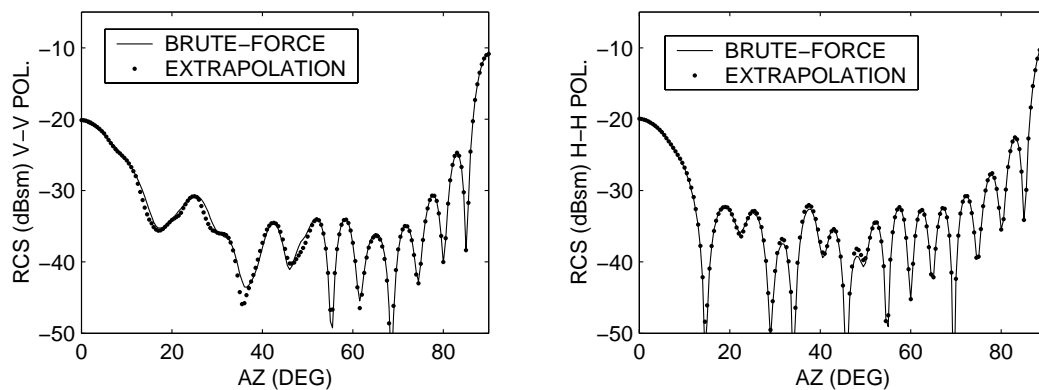


Figure 8. The mono-static RCS of dielectric slab calculated by brute-force, and by extrapolation. The number of RCS points is 181, and the number of samples is 13 for the extrapolation.

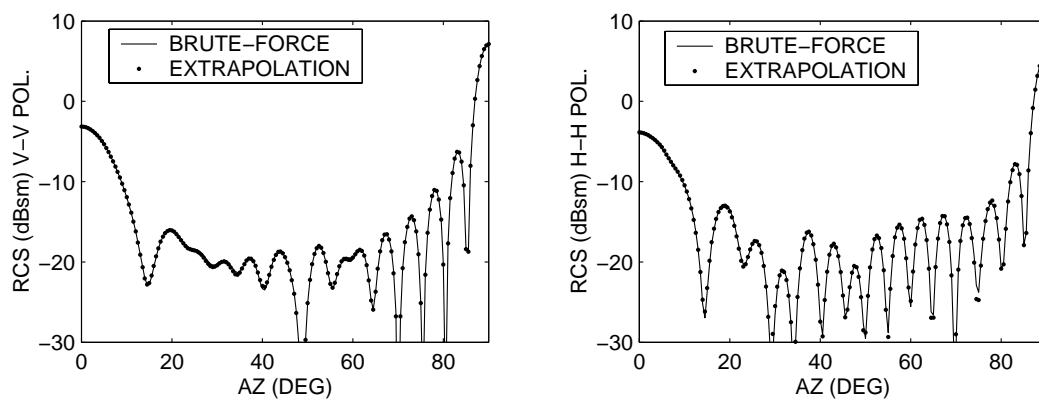


Figure 9. The mono-static RCS of a conducting box coated by a layer of dielectric slab calculated by brute-force, and by extrapolation. The number of RCS points is 181, and the number of samples is 13 for the extrapolation.

IV. Discussions and Summary

There are some remarks that must be pointed out for this method. First, in section 2 above, it has been assumed that the interactions among the basis functions are typically strong when they are close, and are weak when they are far away from each other. This assumption is not valid if there are strong multi-bounce contributions to the far-field. An example is a single 90 degree corner reflector (or aligned array of such reflectors). It has strong two bounce interactions that contribute directly to the backscattered field. Another example is a deep cavity which has multiple wave bounces inside the interior walls. As a result, the simple current extrapolation method introduced above does not apply to these two types of targets. Secondly, as is seen in the numerical example, the CPU time saving does not necessarily proportional to the ratio between the numbers of actual output points and the samples. This is due to the use of the current solution as initial guess to predict the next near-by solutions. In an iterative solver, the number of iterations is normally small if a better initial guess is built. When the output points (angle and frequency) are close, then the solutions are expected to be close as well. As a result, the solution at one point can be used as the initial guess for the next (near-by) point. For the brute-force approach, solution is made for each output point. Hence, the "distance" between two neighbor points is much smaller than that of the samples in the extrapolation method, leading to a smaller number of iterations per solution in the brute-force approach. Finally, it is also noted that for the angular loop, the extrapolation method has about the same level of accuracy as the bi-static to mono-static approximation approach.

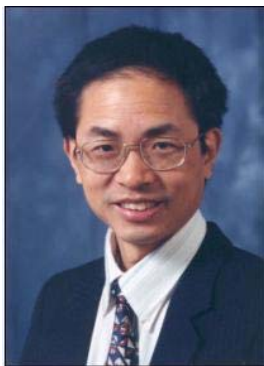
To summarize, a current extrapolation method is introduced to rapidly perform angle and frequency sweep in the far-field calculation using the sparsely sampled solutions. Numerical examples show that the results agree reasonably well to that provided by the direct solution, but the extrapolation method uses about the same amount of memory, and much less CPU time than that of the brute-force approach. There are two advantageous for this method. First, it is easy to implement (no out-of-core processing is needed), and it has small extra memory (in fact, the extra memory required is equal to N complex numbers,

where N is the number of basis functions used in the solution). Secondly, the extrapolation applies to both angle and frequency sweeps.

V. References

- [1] J. M. Song, C. C. Lu, and W.C. Chew, "MLFMA for electromagnetic scattering by large complex objects," *IEEE Trans. Antennas Propagat.*, vol. 45, no. 10, pp. 1488-1493, Oct. 1997.
- [2] Y. Wang and H. Ling, "RCS interpolation in frequency and angle using adaptive feature extraction," *1999 IEEE Int. Antennas Propagat. Symp. Dig.* vol. 37, pp. 450 - 453, June 1999.
- [3] Y. Wang, H. Ling, J. Song, and W. C. Chew, "A frequency extrapolation algorithm for FISC," *IEEE Trans. Antennas Propagat.*, vol. 45, pp. 1891 - 1893, Dec. 1997.
- [4] M. J. Schuh and A. C. Woo, "The monostatic/Bistatic Approximation", *IEEE Antennas and Propagation Magazine*, vol. 36, No. 4, pp. 76-78, Aug. 1994.
- [5] G. J. Burke, E. K. Miller, S. Chakrabarti, K. Demarest, "Using model-based parameter estimation to increase the efficiency of computing electromagnetic transfer functions," *IEEE Trans. Magn.*, vol. 25, pp. 2807 - 2809, July 1989.
- [6] Yuanxun Wang, Hao Ling; "Radar signature prediction using moment method codes via a frequency extrapolation technique," *IEEE Trans. Antennas Propagat.*, vol. 47, pp. 1008 - 1015, June 1999.
- [7] K. Kottapalli, T. K. Sarkar, Y. Hua, E. K. Miller, G. L. Burke, "Accurate computation of wide-band response of electromagnetic systems utilizing narrow-band information," *IEEE Trans. Microwave Theory Tech.*, vol. 39, pp. 682 - 687, Apr. 1991.
- [8] Edward H. Newman, "Generation of wide-band data from the method of moments by interpolating the impedance matrix," *IEEE Trans. Antennas Propagat.*, vol. 36, pp. 1820 - 1824, December 1988.
- [9] Z. Altman and R. Mittra, "A technique for extrapolating numerically rigorous solutions of electromagnetic scattering problems to higher frequencies and their scaling properties," *IEEE Trans. Antennas Propagat.*, vol. 47, pp. 744 - 751, April 1999.

- [10] Y. E. Erdemli, J. Gong, C. J. Reddy, J. L. Volakis, "Fast RCS pattern fill using AWE technique," *IEEE Trans. Antennas Propagat.*, vol. 46, pp. 1752 - 1753, Nov. 1998.
- [11] C. C. Lu and W. C. Chew, "A coupled integral equation technique for the calculation of electromagnetic scattering from composite metallic and dielectric targets," *IEEE Trans. Antenna Propagat.*, vol. 48, no. 12, pp. 1866-1868, Dec. 2000



Dr. Cai-Cheng Lu got his Ph.D. degree from University of Illinois at Urbana-Champaign in 1995, and now he is an associate professor in the Department of Electrical and Computer Engineering at the University of Kentucky. Prior to join University of Kentucky, he was with Demaco, Inc. (now SAIC). His research interests are in wave scattering, microwave circuit simulation, and antenna analysis, and is one of the authors for a CEM code FISC. He is a recipient of the 2000 Young Investigator Award from the Office of Naval Research, and a CAREER Award from the National Science Foundation. Dr. Lu is a senior member of IEEE.